Using the 2011 M_w 9.0 off the Pacific coast of Tohoku Earthquake to test the Coulomb stress triggering hypothesis and to calculate faults brought closer to failure

Shinji Toda[1], Jian Lin[2], and Ross S. Stein[3]

[1]*Disaster Prevention Research Institute, Kyoto University, Japan*
[2]*Woods Hole Oceanographic Institution, Woods Hole, Massachusetts, USA*
[3]*U.S. Geological Survey, Menlo Park, California, USA*

(Received April 7, 2011; Revised May 11, 2011; Accepted May 13, 2011; Online published September 27, 2011)

The 11 March 2011 Tohoku Earthquake provides an unprecedented test of the extent to which Coulomb stress transfer governs the triggering of aftershocks. During 11–31 March, there were 177 aftershocks with focal mechanisms, and so the Coulomb stress change imparted by the rupture can be resolved on the aftershock nodal planes to learn whether they were brought closer to failure. Numerous source models for the mainshock have been inverted from seismic, geodetic, and tsunami observations. Here, we show that, among six tested source models, there is a mean 47% gain in positively-stressed aftershock mechanisms over that for the background (1997–10 March 2011) earthquakes, which serve as the control group. An aftershock fault friction of 0.4 is found to fit the data better than 0.0 or 0.8, and among all the tested models, Wei and Sladen (2011) produced the largest gain, 63%. We also calculate that at least 5 of the seven large, exotic, or remote aftershocks were brought $\geq$0.3 bars closer to failure. With these tests as confirmation, we calculate that large sections of the Japan trench megathrust, the outer trench slope normal faults, the Kanto fragment beneath Tokyo, and the Itoigawa-Shizuoka Tectonic Line, were also brought $\geq$0.3 bars closer to failure.

Key words: Coulomb stress change, Tohoku Earthquake, stress triggering, remote aftershocks.

1. Introduction

The 2011 $M = 9.0$ off the Pacific coast of Tohoku (hereafter, '2011 Tohoku') Earthquake is unprecedented in size in Japan's long recorded history of earthquakes, although some foresaw its possibility (Kanamori *et al*., 2006; McCaffrey, 2008). The earthquake struck on the Japan trench megathrust, which accommodates ~80 mm/yr of convergence. Thanks to Japan's superb monitoring networks, the earthquake is the best-recorded great event the world has ever known. Seismic, geodetic and tsunami observations not only permit detailed source inversions for the distribution of slip on the megathrust surface, but also provide an unparalleled set of aftershocks, which the NIED has used to calculate focal mechanisms for $M \geq 3.5$ events recorded by F-net. Further, the extensive geomorphic, geodetic and paleoseismic analysis of Japan's faults enables us to calculate how the Tohoku Earthquake changed the conditions for failure on surrounding faults.

2. The Coulomb Stress Triggering Hypothesis

An earthquake fault rupture permanently deforms the surrounding crust, changing the stress on nearby faults as a function of their location, geometry and sense of slip (rake). The Coulomb stress change is defined as $\Delta\mathrm{CFF} = \Delta\tau + \mu\Delta\sigma$, where τ is the shear stress on the fault (positive in the inferred direction of slip), σ is the normal stress (positive for fault unclamping), and μ is the apparent friction coefficient. Failure is promoted if ΔCFF is positive, and inhibited if negative; both increased shear and unclamping of faults are taken to promote failure, with the role of unclamping modulated by fault friction. Most investigations of Coulomb stress triggering (Harris, 1998; Stein, 1999; Freed, 2005) find that static stress change plays an important role in the production of aftershocks and subsequent mainshocks on surrounding faults.

3. Test Design

While there is abundant evidence that aftershocks locate in regions of calculated stress increase (the stress triggering lobes) for assumed 'receiver fault' geometries, a stricter test of the Coulomb hypothesis is whether the nodal planes of the aftershocks are promoted for failure. By resolving the Coulomb stress change on aftershock nodal planes in their rake directions, one need not make any assumptions about the aftershock fault geometry or the regional stress. But while the shear stress on the two orthogonal nodal planes is the same, the unclamping stress is different. So, except for the special case of zero fault friction, the Coulomb stress imparted to the two nodal planes will differ, and, except under unusual circumstances, we do not know which of the two planes slipped. Thus, to conduct this test, we resolve the Coulomb stress change on both nodal planes of each mechanism, and use both resulting stress changes in the

Copyright © The Society of Geomagnetism and Earth, Planetary and Space Sciences (SGEPSS); The Seismological Society of Japan; The Volcanological Society of Japan; The Geodetic Society of Japan; The Japanese Society for Planetary Sciences; TERRAPUB.

doi:10.5047/eps.2011.05.010

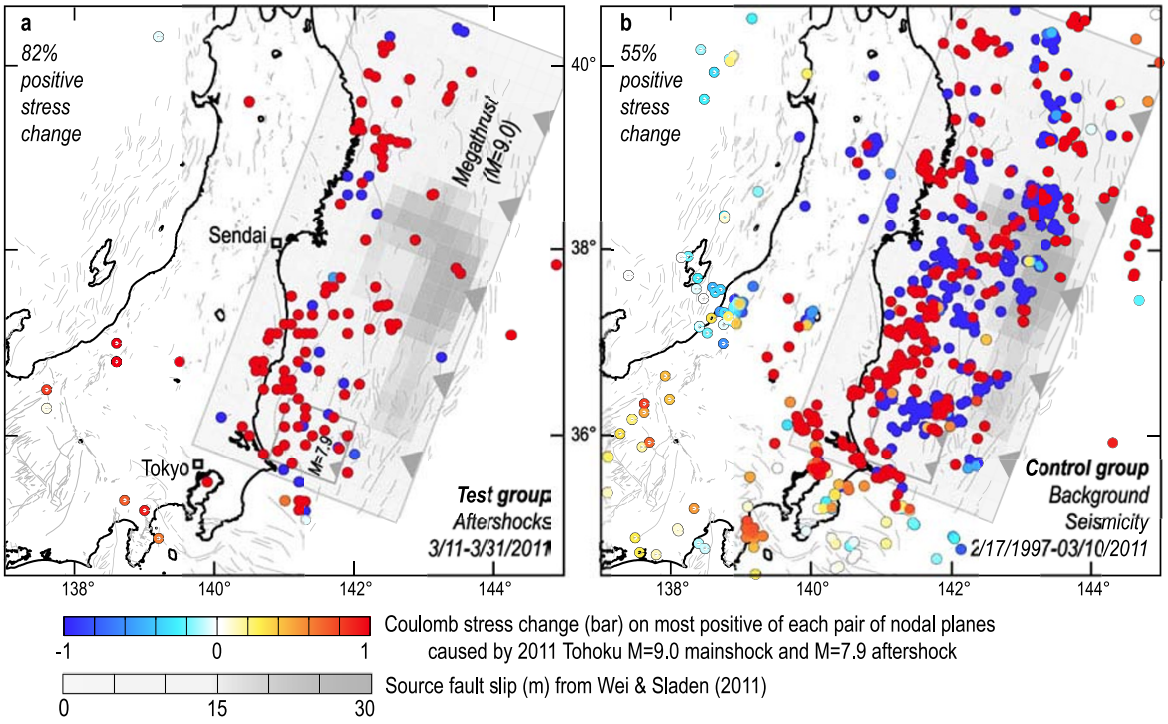

Fig. 1. Stress imparted by the Wei and Sladen (2011) source model and the $M_w = 7.9$ aftershock is resolved on both nodal planes of NIED F-net aftershock (a) and background, or pre-Tohoku (b) focal mechanisms. Although both planes are used for the calculations summarized in Table 1, the most positively-stressed of each pair of nodal planes is shown here. The effect of the mainshock stress imparted to the mechanisms is judged from the percent gain in positively-stressed mechanisms after the mainshock (the test group) relative to the background shocks (the control group). Results for all 6 models are given in Table 1.

statistical sample. This means that because of the nodal plane ambiguity, even if all aftershocks were brought closer to failure, we would never find a 100% agreement.

But even if we found that a majority of aftershock nodal planes were brought closer to failure by the mainshock rupture, this would not necessarily demonstrate that stress transfer was responsible. It is possible that shocks that occurred before the mainshock rupture in the same region would yield a similar percentage, principally because faults that slip during aftershocks might share the same geometry as those that slip at other times. Therefore, the percentage of positively-stressed aftershocks must be normalized by the positively-stressed background shocks. For the 'background,' we use shocks that occurred before the mainshock. In testing terminology, the aftershocks comprise the 'test group,' and the background shocks the 'control group.' What is important is the percentage gain in positively-stressed aftershocks relative to the background shocks, with the background shocks selected to match the geographic area and depth range as the aftershocks. This procedure, first used by Hardebeck *et al.* (1998), is analogous to pharmaceutical testing, in which to prove efficacy, the drug given to the test group must outperform a placebo administered to the control group.

It has proven difficult to discriminate among possible values of fault friction in Coulomb stress transfer studies, and so a mid-value of 0.4 is most commonly adopted. On creeping faults, low friction has been found to fit best, whereas on young thrust and normal faults, a high value of friction may be superior (Parsons *et al.*, 1999; Toda and Stein, 2002). Because of the quality of the test data for the 2011 Tohoku Earthquake, we test three values of fault friction (0.0, 0.4, and 0.8) for each source model, seeking the value that produces the highest gain.

To graphically represent the results economically, we plot the most positive stress change of each pair of nodal planes in Fig. 1, with the convention that where aftershocks overlap, the most positively-stressed shocks are plotted on top. This schema is used for both the aftershocks (Fig. 1(a)) and the background shocks (Fig. 1(b)); this 'positive bias' is only in the figure; stress on both planes are used in all calculations, as summarized in Table 1. We performed all calculations using Coulomb 3.2 (http://www.coulombstress.org).

4. Aftershock Data and Source Models

We use the 177 NIED F-net aftershock focal mechanisms between 11 and 31 March 2011; all are $M \geq 3.5$ events within the depth range of 0–80 km, bounded by 34.5–41.0°N latitude and 137–145°E longitude (Fig. 1(a)). For the background earthquakes, we restricted our search area and depths to the same range as the aftershocks and sought a dataset about five times larger than the aftershocks for statistical confidence; we used 840 $M \geq 4.5$ NIED F-net focal mechanisms during 17 February 1997–10 March 2011 (Fig. 1(b)). We chose $M \geq 4.5$ to limit the size of the sample, and because larger earthquakes likely have more accurate focal mechanisms.

We tested six source models of the 11 March 2011 mainshock that span the range of the assumed megathrust dips (9–15°) and datasets used in the source inversions (tele-

Table 1.

Source model [1] (2011 citation)	Ver.	Moment E^{29} dyn-cm	Dip (°)	Slip patches	Data [2]	% aftershocks with +ΔCFF [3] fric.=0.0	fric.=0.4	fric.=0.8	% background with +ΔCFF [4] fric.=0.0	fric.=0.4	fric.=0.8	Stress effect of mainshock (% gain) [5] fric.=0.0	fric.=0.4	fric.=0.8	Model means
Yagi	v.2	4.5	15	264	a	63	67	69	45	45.8	48.6	56.6	52.9	40.6	50.0
Hayes	v.2	4.9	10.2	325	b	74	76	73	51.5	49.8	51.8	40.0	46.3	42.0	42.8
Shao *et al.*	v.3	5.7	10	190	b	64	63	61	45.5	41.2	43.4	43.7	52.6	40.9	45.7
Fujii and Satake	v.1	2.8	14	25	c	77	81	82	55.7	55.8	56.6	38.2	45.2	44.9	42.8
Wei and Sladen	v.1	4.5	9	350	b, d	73	74	74	50.2	45.5	47.5	45.4	**62.6**	55.8	54.6
Pollitz and Burgmann	v.1	3.6	14	446	d, e	68	67	68	42.1	43.9	51.9	61.5	52.6	31.0	48.4
											Friction means:	47.6	52.0	42.5	47.4

Notes:
[1] $M_w = 7.9$ aftershock included as a source (uniformly tapered with 5 patches from this study, based on Global CMT parameters and ARIA GPS; $M_o = 8.5E^{27}$ dyn-cm)
[2] a, teleseismic body waves; b, teleseismic *P*, *SH*, and long period surface waves; c, DART tsunamigrams and tide gauges; d, static GPS; e, smoothed from 15,876 patches
[3] 176 aftershocks used from NIED F-net database for 3/11/2011–3/31/2011 (all are $M \geq 3.5$, 0–80 km depth, and lie within lat. 34.5–41.0°N, lon. 137–145°E
[4] 840 background shocks from NIED F-net database for 2/17/1997–3/10/2011 (selection criteria: $M \geq 4.5$, 0–80 km depth, lat. 34.5–41.0°N, lon. 137–145°E)
[5] Stress effect of mainshock = [100*(% aftershocks positively stressed by mainshock/% background mechanisms positively stressed by mainshock) − 100];
so if 0%, there is no effect of the rupture on aftershock mechanisms, and if 100%, aftershock mechanisms are promoted at twice the background rate.

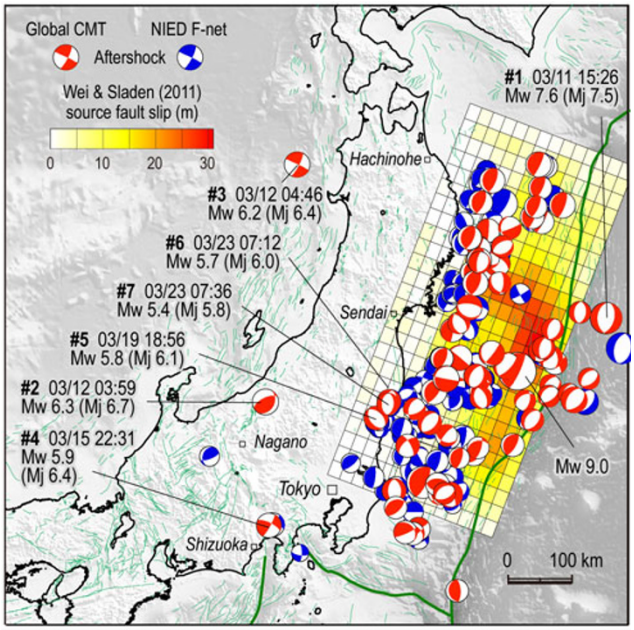

Fig. 2. Focal mechanisms of the March 2011 Tohoku Earthquake aftershocks from two catalogs, with important aftershocks examined for stress transfer keyed to Table 2. The mainshock promotes failure of five of the seven events regardless of nodal plane or friction; for the remaining two events (#1–2) only one of the nodal planes is promoted (see Table 2). All aftershocks east of the mainshock are outer trench slope normal events, but there is also a group of coastal normal events midway between Tokyo and Sendai.

seismic *P*, *SH*, body, and long period surface waves; static GPS displacements; tsunamigrams and coastal tide gauge records), as noted in Table 1. First, we use the combined statistics for all models to test the Coulomb hypothesis and to find the best value of fault friction. We then use the test to discriminate among the candidate models, with the expectation that the source model producing the highest gain in positively-stressed aftershocks relative to background shocks will provide the best estimates of which major surrounding faults have been brought closer to failure by the 2011 Tohoku Earthquake.

5. Test Results and Their Implications

The mean gain in the percentage of positively-stressed aftershocks with respect to the background shocks for all six source models is 47% (47% more aftershocks are brought closer to failure than the control group). We find a friction of 0.4 yields a 5–10% higher gain than for low or high friction (Table 1). Since some aftershocks locate on or near the megathrust surface and others locate in the outer trench slope or on continental faults (Fig. 1(a)), the 0.4 preference could simply be due to averaging different fault strengths. Among the candidate source models, Wei and Sladen (2011) (Figs. 1 and 2) has the highest mean gain for all values of friction (55%); it has the highest gain of all (63%), obtained for friction = 0.4. We thus adopt this model and friction for the remaining tests, and for calculations of stress transfer to surrounding faults. Although many of the aftershocks are on the megathrust, only 6% of the stress changes exceed |50 bar| and so proximity to the rupture surface does not strongly influence the results.

In a similar test, Hardebeck *et al.* (1998) found a 37% gain for immediate aftershocks of the 1992 $M = 7.3$ Landers, California, earthquake, and 46% gain after 3 years. Ma *et al.* (2005) found a gain of 61% (70% for thrust and a 56% gain for strike-slip events) for the 1999 $M = 7.6$ Chi-Chi, Taiwan, earthquake, using a 4-yr-long aftershock period. These studies tested only a single source model and were unable to discriminate among friction values. Because they lack a sufficient number of pre-mainshock focal mechanisms, such tests have not been conducted for the 2004 $M = 9.1$ Sumatra, 2008 $M = 7.9$ Wenchuan, and 2010 $M = 8.8$ Chile, earthquakes.

We next examine the Coulomb stress triggering to the largest, most exotic, and remote aftershocks. For this test, we use the Global CMT catalog, which is more complete than the NIED F-net catalog during the first day after the mainshock. The events include the $M_w = 7.6$ outer trench slope aftershock, several shallow coastal and offshore $5.4 \leq M_w \leq 5.8$ normal events, the thrust event near Nagano, and the remote strike-slip events in the Japan Sea and at the base of Mt. Fuji (Fig. 2). We find that all but the Nagano event (aftershock #2 in Fig. 2 and Table 2) are brought $\geq$0.3 bars closer to failure on at least one nodal plane, and that 4 of the 7 are brought closer to failure on both nodal planes. Thus, the Nagano event does not appear to be statically triggered. 0.3 bar is about 0.25% of the 2011 Tohoku Earthquake stress drop of $\sim$120 bar for the Wei and Sladen (2011) model, and about three times larger than the minimum stress typically found to cause changes in seismicity rates (Stein, 1999).

6. Stress Changes Calculated on Major Faults in Central Japan

Emboldened by the success of the Coulomb hypothesis test for aftershocks, we next calculate the Coulomb stress changes on all known major faults in Fig. 3 to develop insights as to which fault systems are now more hazardous than they were before the 2011 Tohoku Earthquake. We nevertheless caution that the calculation idealizes stress transfer because smaller faults need not share the same geometry as the major faults sampled here, and the dip and rake of even major faults are often poorly known.

On the megathrust surface (which is rather unrealistically represented as a plane in all Tohoku source models), there are large stress increases at depths greater than 35 km, which could give rise to aftershocks and postseismic slip. To the north of the Tohoku rupture in the Sanriku-Hokubu-oki area, there are also large stress increases at depths greater than 30–35 km (Fig. 3). This section hosted the 1994 $M = 7.5$, 1901 $M = 7.4$, 1931 $M = 7.6$, and 1968 $M = 7.9$ and 7.5 earthquakes (south to north, respectively). To the south of the Tohoku rupture lies the Off-Boso section (Fig. 3), which exhibits repeating earthquakes, aseismic slip transients, and possibly uncoupled behavior (Nishimura *et al.*, 2006; Ozawa *et al.*, 2007). Despite this, there have been 2 $M > 6$ and 4–5 $M \geq 5$ Off-Boso aftershocks of the 2011 Tohoku Earthquake (Fig. 2), and so it must also store elastic stress. Stress increases of about 10 bars are calculated along the northern margin of the Off-Boso section of the Japan trench adjacent to the $M_w = 7.9$ aftershock, declin-

Table 2.

#	Occurrence time (local time) mo/dy/yr hr:mn	Lon. (°)	Lat. (°)	Depth (km)	M_w	M_j	strike NP1 (°)	dip NP1 (°)	rake NP1 (°)	normal stress (bar)	shear stress (bar)	Coulomb stress $\mu = 0.4$ (bar)	Coulomb stress $\mu = 0.8$ (bar)	strike NP2 (°)	dip NP2 (°)	rake NP2 (°)	normal stress (bar)	shear stress (bar)	Coulomb stress $\mu = 0.4$ (bar)	Coulomb stress $\mu = 0.8$ (bar)
1	2011.3.11 15:26	144.63	38.27	21.1	7.6	7.5	182	42	−100	**−9.3**	**2.2**	**−1.5**	**−5.2**	15	49	−81	**4.9**	**2.2**	**4.1**	**6.1**
2	2011.3.12 3:59	138.59	37.08	12.0	6.3	6.7	28	33	58	**0.7**	**−0.3**	**0.0**	**0.3**	244	63	109	**0.1**	**−0.3**	**−0.3**	**−0.2**
3	2011.3.12 4:46	139.15	40.4	12.0	6.2	6.4	27	78	−177	**1.9**	**0.5**	**1.2**	**2.0**	296	87	−12	**0.0**	**0.5**	**0.5**	**0.5**
4	2011.3.15 22:31	138.65	35.29	17.7	5.9	6.4	296	70	172	**0.7**	**0.4**	**0.6**	**0.9**	29	82	20	**−0.1**	**0.4**	**0.3**	**0.3**
5	2011.3.19 18:56	140.55	36.85	12.0	5.8	6.1	146	44	−81	**3.2**	**3.9**	**5.1**	**6.4**	314	47	−98	**3.3**	**3.9**	**5.2**	**6.5**
6	2011.3.23 7:12	140.78	37.09	12.0	5.7	6.0	15	37	−92	**5.4**	**6.6**	**8.8**	**11.0**	197	53	−89	**9.0**	**6.6**	**10.2**	**13.8**
7	2011.3.23 7:36	140.76	37.05	12.4	5.4	5.8	182	42	−92	**6.4**	**7.1**	**9.7**	**12.3**	5	48	−88	**8.3**	**7.1**	**10.4**	**13.8**

Wei and Sladen (2011) plus the $M_w = 7.9$ aftershock model from this study are used as sources. M_j is JMA magnitude. NP1 = Nodal Plane 1, etc. μ = friction coefficient.

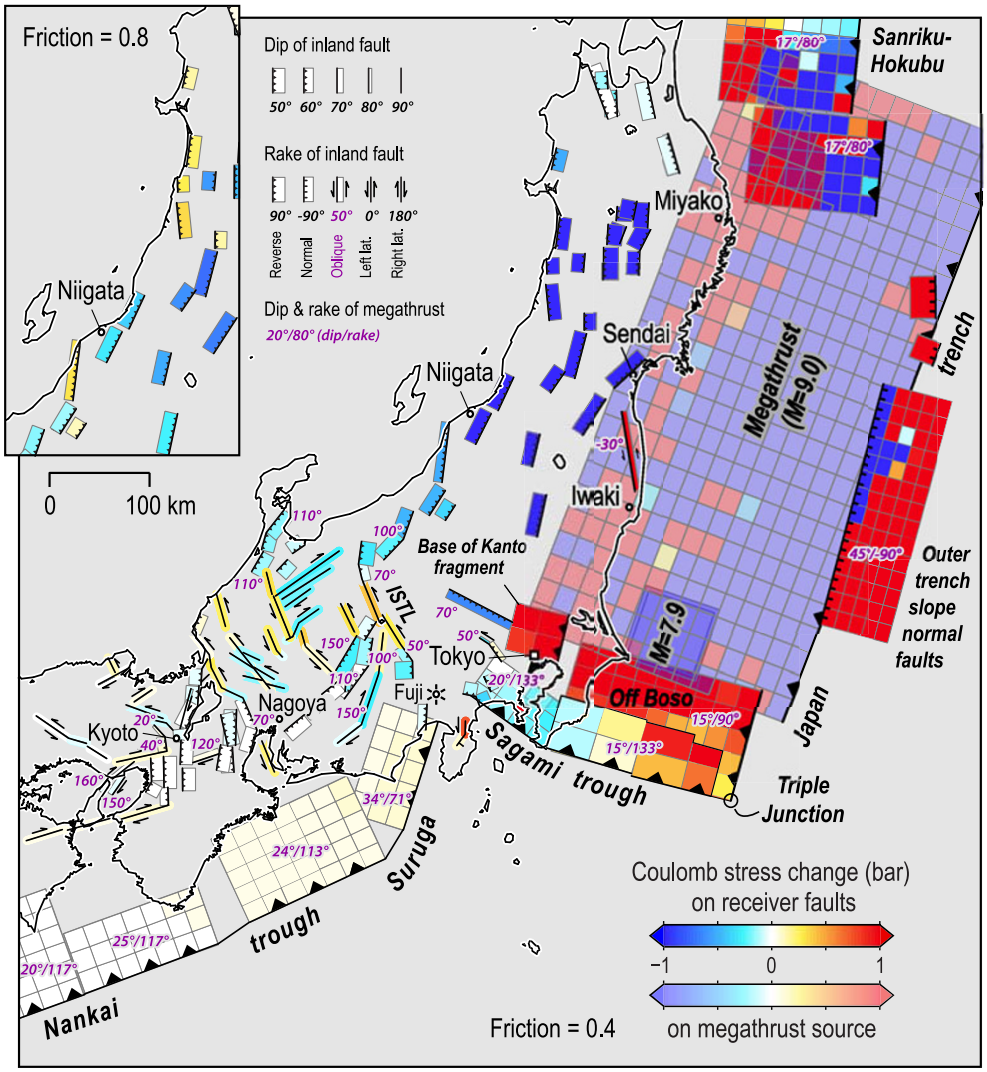

Fig. 3. Stress imparted by the Wei and Sladen (2011) source model and the $M_w = 7.9$ aftershock to surrounding active faults (Research Group for Active Faults in Japan, 1991; Headquarters for Earthquake Research Promotion, 2011), resolved in their inferred rake directions (oblique rakes are labeled). Top and bottom depths of most of the active faults are set to 0 and 15 km.

ing to 0.3 bars to the south. If this entire 100- by 180-km section ruptured, it could host a $M = 8.1$ earthquake, and so we believe that such a possibility cannot be dismissed even though no such event is evident in the historical record (Grunewald and Stein, 2006).

The sections of the Sagami trough that last ruptured in the 1923 $M = 7.9$ Kanto event (Nyst *et al.*, 2006) are calculated to experience Coulomb stress decreases of 0.2–0.5 bar by the 2011 Tohoku Earthquake, whereas the stress increased by 0.5–1.0 bar on the easternmost section. The stressed sections might have participated in the 31 December, 1703, $M \sim 8.2$ Genroku and 4 November, 1677, $M \sim 8$? tsunamigenic earthquakes (Grunewald and Stein, 2006). The Suruga trough megathrust (Ando, 1975; Ishibashi, 1981), site of the 1854 $M = 8.4$ event, was brought a negligible 0.02–0.07 bars closer to failure since it is not much larger than the 0.01-bar Coulomb stresses induced by the tides. The left-lateral Itoigawa-Shizuoka Tectonic Line (ISTL), as well as many parallel faults to the west of it, were brought 0.3–0.4 bar closer to failure. For a fault friction of 0.4, the major thrust faults of Tohoku were inhibited from failure by 1 bar. However, for a high value of friction that might be more appropriate for youthful thrust continental thrusts (Parsons *et al.*, 1999), some Tohoku thrusts are unclamped, leading to Coulomb stress increases of 0.1–0.4 bar (see Fig. 3 inset). In contrast to the Tohoku thrusts, failure is promoted on outer trench slope normal faults by 1.5–15 bars, depending on their proximity to the locus of high slip. Numerous large Tohoku outer trench slope normal aftershocks have struck here since the Tohoku mainshock, including the 11 March, 2011, $M_w = 7.6$ event (Fig. 2). The largest outer rise event in this region was the 3 March, 1933, $M = 8.1$ quake, whose tsunami inundated the Sanriku coast (Kanamori, 1971). The southern 2/3 of the likely 1933 rupture zone (long red rectangle near the trench in Fig. 3) was brought 6 bars closer to failure.

The 'Kanto fragment' was proposed by Toda *et al.* (2008) to explain the seismic tomography, microseismicity, geodetic deformation and plate motion evolution of the Philippine Sea and Pacific slab interaction beneath Tokyo. They argued that the fragment broke off the Pacific slab and is wedged between the Pacific and Philippine Sea slabs and

the over-riding Eurasian plate. We calculate that the 60–80-km-deep base of the fragment has been brought 1–2 bars closer to failure, whereas the upper surface, in contact with the Philippine Sea slab, has been brought 0.3 bars closer to failure. If the entire lower surface of the fragment were to rupture, a $M = 7.3$ event could strike at ∼75 km depth beneath the highly-populated Kanto basin.

7. Conclusions

We have sought to conduct the most rigorous test possible of the Coulomb failure hypothesis that can be applied to the 2011 Tohoku Earthquake less than one month after the mainshock. The test is made feasible by the extraordinary quality and accessibility of the Japanese seismic and geodetic monitoring networks, and by scientists openly sharing their preliminary source models, for which we are grateful. We find that all source models yield at least a 43% gain in positively-stressed aftershock nodal planes relative to the nodal planes of background seismicity, and the best tested model yields a 63% gain, the highest yet seen for any earthquake tested. When this model is used to examine the seven remote, exotic, and largest aftershocks, at least one nodal plane of six of these is brought >0.3 bar closer to failure, and so the remote aftershocks can have the same static-stress origin as those on the rupture surface. Examining all major fault systems in central Japan, large stress increases are calculated to the north and south and along the base of the Tohoku megathrust rupture surface, on outer trench slope normal faults, on the easternmost sections of the Sagami trough megathrust, along the ISTL and subparallel faults, and on the base of the Kanto fragment that, we believe, underlies Tokyo.

Acknowledgments. We thank Volkan Sevilgen for technical assistance; Meredith Nettles for Global CMT analyses; Yuji Yagi, Gavin Hayes, and Chen Ji for source modeling insights; and David Shelly and Fred Pollitz for thoughtful and rapid reviews.

References

Ando, M., Source mechanisms and tectonic significance of historic earthquakes along the Nankai trough, *Tectonophysics*, **22**, 173–186, 1975.

Freed, A. M., Earthquake triggering by static, dynamic, and postseismic stress transfer, *Ann. Rev. Earth Planet. Sci.*, **33**, 335–367, doi: 310.1146/annurev.earth.1133.092203.122505, 2005.

Grunewald, E. and R. S. Stein, A new 1649–1884 catalog of destructive earthquakes near Tokyo and implications for the long-term seismic process, *J. Geophys. Res.*, **111**, doi:10.1029/2005JB004059, 2006.

Hardebeck, J. L., J. J. Nazareth, and E. Hauksson, The static stress change triggering model: Constraints from two southern California aftershocks sequences, *J. Geophys. Res.*, **103**, 24,427–24,437, 1998.

Harris, R. A., Introduction to special section: Stress triggers, stress shadows, and implications for seismic hazard, *J. Geophys. Res.*, **103**, 24,347–24,358, 1998.

Headquarters for Earthquake Research Promotion, Long-term evaluation of active faults, http://www.jishin.go.jp/main/p_hyoka02_danso.htm, 2011.

Ishibashi, K., Specification of soon-to-occur seismic faulting in the Tokai district, central Japan, based upon seismotectonics, in *Earthquake Prediction—An International Review*, edited by D. W. Simpson and P. G. Richards, pp. 297–332, Amer. Geophys. Un., Wash., D.C., 1981.

Kanamori, H., Seismological evidence for a lithospheric normal faulting—the Sanriku earthquake of 1933, *Phys. Earth Planet. Inter.*, **4**, 289–300, 1971.

Kanamori, H., M. Miyazawa, and J. Mori, Investigation of the earthquake sequence off Miyagi prefecture with historical seismograms, *Earth Planets Space*, **58**, 1533–1541, 2006.

Ma, K.-F., C.-H. Chan, and R. S. Stein, Response of seismicity to Coulomb stress triggers and shadows of the 1999 Mw=7.6 Chi-Chi, Taiwan, earthquake, *J. Geophys. Res.*, **110**, doi:10.1029/2004JB003389, 2005.

McCaffrey, R., Global frequency of magnitude 9 earthquakes, *Geology*, **8**, 263–266, doi:10.1130/G24402A.1, 2008.

Nishimura, T., T. Sagiya, and R. S. Stein, Crustal block kinematics and seismic potential of the northernmost Philippine Sea plate and Izu microplate, central Japan, inferred from GPS and leveling data, *J. Geophys. Res.*, **112**, doi:10.1029/2005JB004102, 2006.

Nyst, M., T. Nishimura, F. F. Pollitz, and W. Thatcher, The 1923 Kanto earthquake re-evaluated using a newly augmented geodetic data set, *J. Geophys. Res.*, **111**, B11306, doi:11310.11029/12005JB003628, 2006.

Ozawa, S., H. Suito, and M. Tobita, Occurrence of quasi-periodic slow-slip off the east coast of the Boso peninsula, Central Japan, *Earth Planets Space*, **59**, 1241–1245, 2007.

Parsons, T., R. S. Stein, R. W. Simpson, and P. A. Reasenberg, Stress sensitivity of fault seismicity: A comparison between limited-offset oblique and major strike-slip faults, *J. Geophys. Res.*, **104**, 20,183–20,202, 1999.

Research Group for Active Faults in Japan, *Active Faults in Japan, Sheet Maps and Inventories*, rev. ed., 437 pp., Univ. Tokyo Press, Tokyo, 1991.

Stein, R. S., The role of stress transfer in earthquake occurrence, *Nature*, **402**, 605–609, 1999.

Toda, S. and R. S. Stein, Response of the San Andreas fault to the 1983 Coalinga-Nuñez Earthquakes: An application of interaction-based probabilities for Parkfield, *J. Geophys. Res.*, **107**, doi:10.1029/2001JB000172, 2002.

Toda, S., R. S. Stein, S. H. Kirby, and S. B. Bozkurt, A slab fragment wedged under Tokyo and its tectonic and seismic implications, *Nature Geosci.*, **1**, 1–6, doi:10.1038/ngeo1318, 2008.

Wei, S., A. Sladen, and the ARIA project, 2011 Tohoku source model v.1, http://www.tectonics.caltech.edu/slip_history/2011_taiheiyo-oki/, 2011.

S. Toda (e-mail: toda@rcep.dpri.kyoto-u.ac.jp), J. Lin, and R. S. Stein